20th Annual International Conference on Mechanical Engineering-ISME2012
16-18 May, 2012, School of Mechanical Eng., Shiraz University, Shiraz, Iran

ISME2012-3371

Numerical Simulation of Cavitation around a Two-Dimensional Hydrofoil Using LES

Amir Pouyan Zahiri[1], Ehsan Roohi[2], Mahmud Pasandideh-fard[3]

[1] M.Sc. Student, Ferdowsi university of Mashhad; pooyan.zahiri@yahoo.com
[2] Assistant Professor, Ferdowsi university of Mashhad; e.roohi@um.ac.ir
[3] Associate Professor, Ferdowsi university of Mashhad; fard_m@um.ac.ir

SUMMARY
In this paper simulation of cavitating flow over the Clark-Y hydrofoil is reported using computational fluid dynamics (CFD) technique. This simulation is performed using the large eddy simulation (LES) turbulence model. We applied an incompressible LES modeling approach based on an implicit method for the subgrid terms. To apply the cavitation model, the flow has been considered as a single fluid, two-phase mixture. A transport equation model for the local volume fraction of vapor is solved with the LES model and a finite rate mass transfer model is used for the vaporization and condensation processes. The volume of fluid (VOF) method is applied to track the interface of liquid and vapor phases. This simulation is performed using a two phase solver available in the framework of the OpenFOAM (open field operation and Manipulation) software package, namely "interPhaseChangeFoam". The solver is based on the finite volume method. Simulation is performed for the cloud and super cavitation regimes. The results of our simulation are compared with the experimental data and the accuracy of the simulation has been investigated.

Keywords: Clark-Y hydrofoil, cloud cavitation, supercavitation, LES, mass transfer mode.

Introduction

Formation of vapor bubbles within a liquid when its pressure is less than the saturated vapor pressure is called cavitation. The cavitation usually could appear over marine vehicles such as marine propeller blades. For efficiency reasons, the propeller usually needs to be operated in cavitating conditions but one still needs to avoid the negative effects of cavitation such as vibrations, noise and erosion. The radial section of these marine blades is a two-dimensional hydrofoil.
The numerical simulation of cavitation phenomenon does however include many complications from modeling and computational point of views. For example, the phase change from liquid to water is difficult to model on a macroscopic level and the cavitation dynamics is governed by medium to small flow scales, both in time and space, necessitating large computational grids and small time steps.
In this research, we validated the ability of large eddy simulation (LES) model to simulate cavitating flow over a tow-dimensional Clark-Y hydrofoil whose experimental data is available [1]. LES is based on computing the large, energy-containing structures that are resolved in the computational grid [2]. A transport equation for the local volume fraction of vapor phase is solved together with the LES equations, and a finite rate mass transfer model is used for the vaporization and condensation processes. According to the literature, there are different mass transfer models such as Sauer, Kunz and Merkle models. In this work, we used Sauer model in our simulation. Volume of fluid (VOF) strategy is applied to track the interface of liquid and vapor phases. VOF model used in the OpenFOAM considers the effect of the surface tension force over the free surface.

Implicit LES Model

Large eddy simulation (LES) is based on computing the large, energy-containing structures that are resolved on the computational grid, whereas the smaller, more isotropic, subgrid structures are modeled. Development of the LES encounters a main obstacle of the strong coupling between subgrid scale (SGS) modeling and the truncation error of the numerical discretization scheme. This link could be exploited by developing discretization methods where the truncation error itself acts as an implicit SGS model. Therefore, the "implicit LES" expression is used to indicate approaches that merge SGS model and numerical discretization [2]. Furthermore, the cell-averaging discretisation of the flow variables can be thought of as an implicit filter. In the other words, finite volume discretization provides top-hat-shaped-kernel filtered values as:

$$\bar{f}_p = \frac{1}{(\delta V_p)} \int_{\Omega_p} f dV \qquad (1)$$

, where over-bar denotes filtered quantity for cell Ω_p and V_p is the volume of the cell.
In the implicit LES approach employed here, the truncation error of the discretization scheme acts as the subgrid modeling. In contrast to RANS approaches, which are based on solving for an ensemble average of the flow properties, LES naturally and consistently allows for medium to small scale, transient flow structures. When simulating unsteady, cavitating flows, we believe this is an important property in order to be able to capture the mechanisms governing the dynamics of the formation and shedding of the cavity [2]. Thus, starting from the incompressible Navier-Stokes equations, the governing flow equations consisting of the balance equations of mass and momentum,

$$\partial_t(\rho v)+\nabla.(\rho v\times v)=-\nabla p+\nabla.s,$$
$$\partial_t\rho+\nabla.(\rho v)=0 \quad (1)$$

, where v is the velocity, p is the pressure, $s = 2\mu D$ is the viscous stress tensor, where the rate-of-strain tensor is expressed as $D=\frac{1}{2}\left(\nabla v+\nabla v^T\right)$ and μ is the viscosity. The LES equations are theoretically derived, following e.g. Sagaut, [3] from Eq. (1) by applying a low-pass filtering G = G(x, Δ), using a pre-defined filter kernel function such that,

$$\partial_t\left(\rho\bar{v}\right)+\nabla.\left(\rho\bar{v}\times\bar{v}\right)=-\nabla\bar{p}+\nabla.\left(\bar{s}-B\right),$$
$$\partial_t\rho+\nabla.\left(\rho\bar{v}\right)=0 \quad (2)$$

As no explicit filtering is employed, commutation errors in the momentum equation have been neglected. Equation (2) introduces one new term when compared to the unfiltered Eq. (1): the unresolved transport term B, which is the sub grid stress tensor. Following Bensow and Fureby [4], B can be exactly decomposed as

$$B=\rho.\left(\overline{\bar{v}\times\bar{v}}-\bar{\bar{v}}\times\bar{\bar{v}}+\tilde{B}\right) \quad (3)$$

, where now only $\tilde{B}$ needs to be modeled. The most common subgrid modeling approaches utilizes an eddy or subgrid viscosity, ν_{SGS}, similar to the turbulent viscosity approach in RANS, where ν_{SGS} can be computed in a wide variety of methods [3]. In the current study, subgrid scale terms are modeled using "one equation eddy viscosity" model.

Multiphase Modeling

To simulate cavitating flows, the two phases of liquid and vapor need to be represented in the problem, as well as the phase transition mechanism between the two. Here, we consider a one fluid, two-phase mixture approach, introduced through the local vapor volume fraction and having the spatial and temporal variation of the vapor fraction described by a transport equation including source terms for the mass transfer rate between the phases. Adding this transport equation to the filtered equations of continuity and momentum given by Eq. (2), we get the following set of equations:

$$\partial_t\left(\rho\bar{v}\right)+\nabla.\left(\rho\bar{v}\times\bar{v}\right)=-\nabla\bar{p}+\nabla.\left(\bar{s}-B\right),$$
$$\partial_t\rho+\nabla.\left(\rho\bar{v}\right)=0,$$
$$\partial_t\alpha+\nabla.\left(\alpha\bar{v}\right)=\dot{m}/\rho_v. \quad (4)$$

The density and viscosity in Eq. 5 are assumed to vary linearly with the vapor fraction,

$$\mu=\mu_v+(1-\alpha)\mu_l, \quad (5)$$

$$\rho=\rho_V+(1-\alpha)\rho_l. \quad (6)$$

Mass Transfer Modeling of Sauer

We had used Sauer model in our simulation. The approach chosen by Sauer [5] is based on expressing the vapor fraction as a function of the number of bubbles per unit volume, n_0, and the radius of the bubbles, R_b, assumed to be the same for all bubble.

$$\dot{m}=-\rho_v(1-\alpha)\frac{\partial\alpha}{R_b}sign\left(\bar{p}-p_v\right)\sqrt{\frac{2}{3}\frac{\left|\bar{p}-p_v\right|}{\rho l}} \quad (7)$$

Simulation Set-up

The computational domain and boundary conditions are given according to the experimental setup in Ref. [1] as shown in Fig 1. The Clark-Y hydrofoil is placed at the center of water tunnel with the angle of attack equal to 8 degree. The two important non-dimensional numbers used are the Reynolds number (Re) and cavitation number σ. The properties of the inlet free stream are used in these numbers defined as bellow:

$$\mathrm{Re}=\frac{U_\infty.c}{\nu} \quad (8)$$

$$\sigma=\frac{p-p_\infty}{\frac{\rho.U_\infty^{\ 2}}{2}} \quad (9)$$

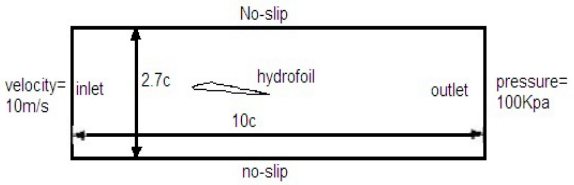

Figure 1: Computational domain and boundary conditions.

, where p is the pressure, p_∞ is free stream vapor pressure and U_∞ is the free stream velocity which is imposed 10 m/s. With the chord length equal to 7 cm, we have σ=0.8 and Re=7×10^5.

Grid Independency Study

As the Clark-Y hydrofoil is not geometrically complex, we used structured quadrilateral meshes. Mesh size near the wall has a key effect on the cavitation frequency and dynamics [6-7]. Meshes are refined in both axial and normal directions to get a cavitation dynamic like the experimental data. The effect of using four different grid sizes on the average pressure profile, over one period of cavitation, on the upper and lower surfaces of the hydrofoil are shown in Fig. 2. Grids 1 to 4 have 65, 130, 270 and 420 cells on the upper surface and 43, 87, 180 and 280 cells on the lower surface of the hydrofoil, respectively. It is observed that the difference between the pressure curves becomes negligible as the number of surface cells increases. Additionally, this figure shows that the grids 3 and 4 provide close solutions, especially for the upper surface, where the cavitation occurs. Therefore, we performed our simulations using grid 3.

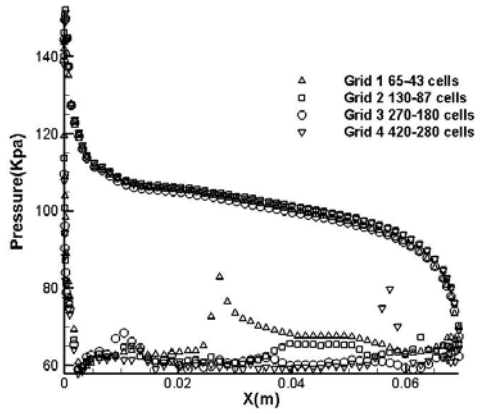

Figure 2: Investigating the effect of different grid sizes on the average pressure profile over the hydrofoil surfaces.

Results and Discussions

Cloud Cavitation

In Fig. 3 the shape and dynamics of cloud cavitation are shown. Left column shows the current simulated cavitation and right column shows the experimental pictures [1]. Pictures are for different non-dimensional time (*t/T*) while *T* is the total period of cavitation period. It shows that the cavitating flow grows till about the midpoint of the cycle, before the massive vortex shedding appears. Afterward, cavitation becomes weaker and finally it separates from the wall and disappears in the fluid flow. As Fig. 3 shows, there are good agreements between the current numerical solutions with those of experiments. This is due to employing complex turbulence model, i.e., LES, in addition to benefiting from VOF technique in reconstructing the free surface.

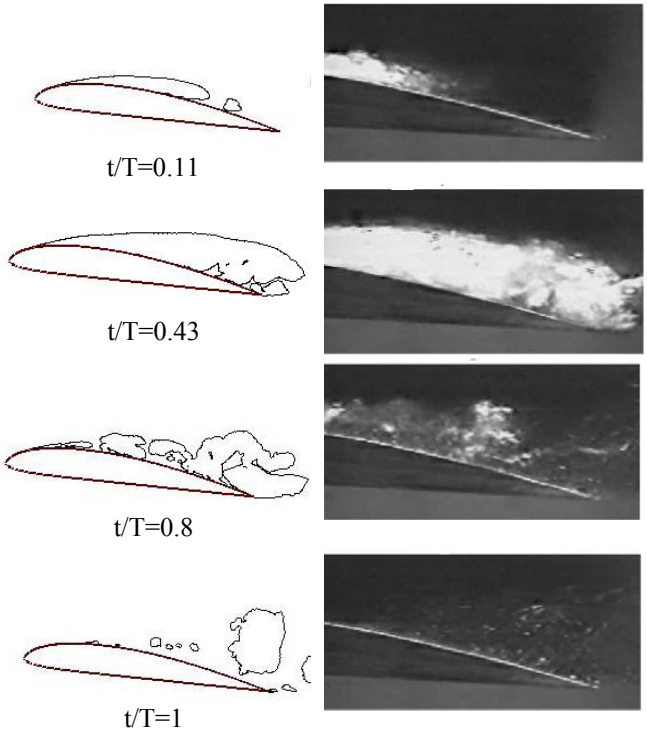

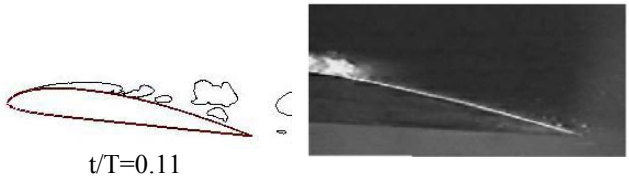

Figure 3: Shape of cavitation from the current simulation and experiment [1] for cloud cavitation regime.

Figures 4 and 5 show the variations of lift and drag coefficients with time. From this curves, we could calculate the average amounts of C_L and C_D. In table 1, the average values of C_L and C_D from our simulation and experimental data are also reported. Simulation results are in good agreement with the experimental data.

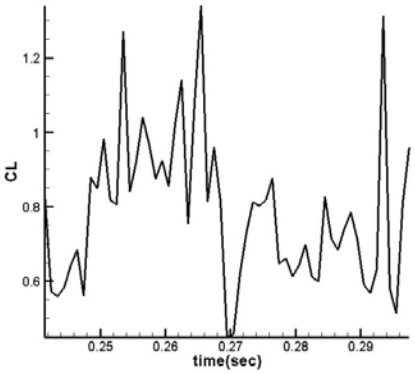

Figure 4: Variation of lift coefficient with time in cloud cavitation.

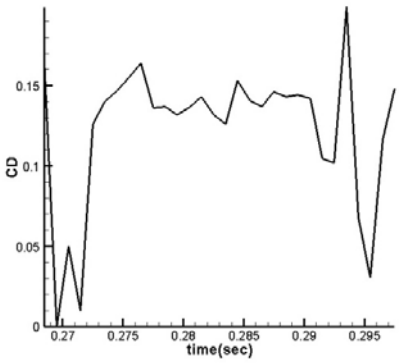

Figure 5: Variation of drag coefficient with time in cloud cavitation.

Table 1: Averages of lift and drag coefficients.

	Cavitation number σ = 0.8	
	experiment	simulation
C_L	0.76	0.71
C_D	0.119	0.122

The velocity profile in the boundary layer of the hydrofoil at location x/c=0.2% is illustrated in Fig. 6 from both of simulation and experiment. This time-averaged velocity profile is tracked along the vertical direction from the hydrofoil wall. Similar to previous results, our simulation is close to the experimental data reported for Clark-Y hydrofoil [1].

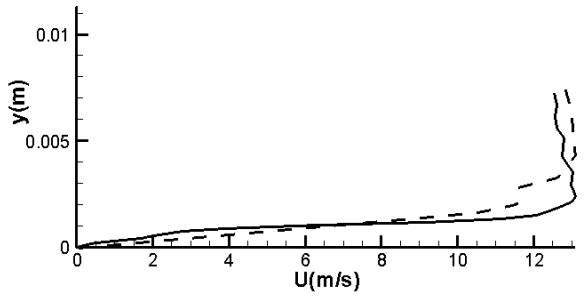

Figure 6: Boundary layer velocity profile at x/c =0.2, black line is the current simulation and dashed line is experimental data [1].

Supercavitation

We also extended our simulations to the supercavitation regime at σ = 0.4. In Fig. 7, the shape of supercavitation from the current simulation (left) and experiment (right) is shown. The mechanism of cavitation growth and vortex shedding is strangely decreased in supercavitation. It is observed that the shape of simulated supercavitation is in good agreement with experimental results.

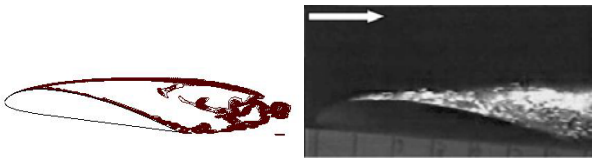

Figure 7: Supercavitation shape from the current simulation (left) and experiment (right) [1] (σ = 0.4).

We also extracted the average amounts of hydrodynamic coefficients (C_L and C_D) for the supercavitation, as reported in table 2. There is good agreement between the current simulation results with those of experimental data [1].

Table 2: Averages of lift and drag coefficients for supercavitation test case.

	Cavitation number σ = 0.4	
	experiment	simulation
C_L	0.30	0.335
C_D	0.075	0.096

Numerical simulation for a supercavitating flow at σ = 0.28 is shown in Fig. 8. In comparison to the previous test case, decreasing the cavitation number resulted in longer vapor region. It should be noted that as the supercavity length and diameter increases, the effects of turbulence instabilities at the closure section decays and more stable cavities are observed.

Figure 8: Supercavitation shape from the current simulation (σ = 0.28).

Conclusion

In the present study, a finite volume solver benefiting from the implicit LES turbulence model and accompanied with the VOF interface capturing method has been employed to capture unsteady cloud cavitation and steady supercavitating flows around the Clark-Y hydrofoil. The Sauer mass transfer model is employed for cavitation modeling. Our simulation show that combination of the LES, VOF and Sauer models has a precise ability to simulate the shape of cloud cavitation and its dynamics. Also lift and drag coefficients are obtained close to the experimental data for both studied regimes.

REFERENCES

[1] Wang, G., Senocak, I., Shyy, W., Ikohagi, T., and Cao, S., 2001. "Dynamics of Attached Turbulent Cavitating Flows". *Progress in Aerospace Sciences*, 37, pp. 551-581.

[2] Bensow, R. E. and Bark, G. 2010, "Simulating cavitating flows with les in openfoam". *V European Conference on Computational Fluid Dynamics,* 14-17 June.

[3] Sagaut P., 2006, "Large Eddy Simulation for Incompressibl Flows". *Springer, New York, 3rd edition.*

[4] Bensow, R. E., and Fureby, C., 2007, "On the Justification and Extension of Mixed Methods in LES". *Journal of Turbulence,* 8.

[5] Sauer, J., 2000, "Instation ren kaviterende Str mung - Ein neues Modell, baserend auf Front Capturing (VoF) and Blasendynamik". *PhD thesis,* Universitat, Karlsruhe.

[6] Goncalvès, G., and Decaix, J., 2011, "Wall Model and Mesh Influence Study for Partial Cavities". *European Journal of Mechanics B/Fluids*, 31(12), pp. 1-18.

[7] Lu, N. X., 2010. "Large Eddy Simulation of Cavitating Flow on Hydrofoils". *licentiate of engineering thesis,* Department of Shipping and Marine Technology, Chalmers University of Technology, Göteborg, Sweden.